

Near Field Pattern Simulations of Graded-Index Multimode Fibres

R.W. Smink, C.P. Tsekrekos, B.P. de Hon, A.M.J. Koonen and A.G. Tjihuis

Eindhoven University of Technology, P.O. Box 513, 5600 MB Eindhoven,
The Netherlands. E-mail: r.w.smink@tue.nl

To compute the near field pattern (NFP) of a silica graded-index multimode fibre, a full-wave model has been implemented. A single-mode fibre pigtail, with possible angular tilt and radial offset, excites the wavefield. The amplitudes of the propagating modes are computed by overlap integrals. The graded-index α -profile has been determined by matching differential mode delay simulations to measurements. Differential mode attenuation and mode-mixing are introduced through a power-flow equation. Only minor parameter adjustments suffice to obtain a satisfactory match between measurements and simulations. To gain a better understanding of the phenomena, NFPs have been determined for a range of excitation positions and angles.

Introduction

In short-range optical communication networks, e.g. in-building networks, the multimode fibre (MMF) is widely accepted as a means to transfer data. In comparison with a single-mode fibre (SMF), the MMF benefits from its large core diameter, since splicing is easier and the use of expensive high-precision connectors is not required. However, the capacity of MMFs regarding their bandwidth is limited due to differential mode delay (DMD). This disadvantage can be mitigated considerably by using a well-chosen graded refractive index-profile in the fibre core. Moreover, by a selective excitation of a subset of propagating modes, the bandwidth can be increased even further, due to reduced propagation time differences [1]. By exciting different subsets simultaneously, parallel independent transmission channels can be created in the MMF, which is a technique known as mode group diversity multiplexing (MGDM) [2].

We have implemented a full-wave model to compute the near field pattern (NFP) at the output of a graded-index multimode fibre (GI-MMF) [3]. A continuous wave laser, pigtailed to a SMF, serves as excitation of the modefield in the GI-MMF. The possibility exists to perform a selective excitation by employing an angular tilt and/or radial offset. We have compared simulated NFPs with measured ones and determined the effects of differential mode attenuation (DMA) and mode-mixing, with the aid of a power flow equation.

Theoretical Investigation

To compute the modal propagation coefficients in the GI-MMF, we assume that the fibre under consideration is circularly symmetric, isotropic and translationally invariant. The fibre consists of a radially inhomogeneous core and an infinite homogeneous cladding. A three-term Sellmeier dispersion equation is used to characterise the permittivity of the fibre material $\epsilon(r, \omega)$, with an $e^{j\omega t}$ time-dependence [4]. A full-vectorial field model has been implemented and the modal electromagnetic fields $\mathbf{E}^{m,n}$ and $\mathbf{H}^{m,n}$, where $m =$

$0, 1, 2, \dots$ and $n = 1, 2, \dots$ denote the azimuthal and radial modal indices, respectively, are determined for each modal propagation coefficient $k_z^{m,n}$. In a cylindrical coordinate system $\{r, \phi, z\}$, with corresponding unit vectors $\{\mathbf{u}_r, \mathbf{u}_\phi, \mathbf{u}_z\}$, the electromagnetic fields in a z -directed fibre can be expressed as

$$\begin{bmatrix} \mathbf{E}(r, \phi, z) \\ \mathbf{H}(r, \phi, z) \end{bmatrix} = \sum_{m,n} A^{m,n} \begin{bmatrix} \mathbf{E}^{m,n}(r) \\ \mathbf{H}^{m,n}(r) \end{bmatrix} e^{-jm\phi} e^{-jk_z^{m,n}z}. \quad (1)$$

The modal fields are normalised to unit power. We excite the GI-MMF at the plane $z = 0$. There, the modal amplitudes $A^{m,n}$ of the corresponding excited modes are determined by an overlap integral [6],

$$A^{m,n} = \frac{1}{2} \int_{r=0}^{\infty} \int_{\phi=-\pi}^{\pi} \mathbf{u}_z \cdot \{ \mathbf{E}^i(r', \phi') \times [\mathbf{H}^{m,n}(r, \phi)]^* \} r d\phi dr, \quad (2)$$

where $\mathbf{E}^i(r', \phi')$ is the electric field of the SMF. The primed coordinates $\{r'(r, \phi), \phi'(r, \phi)\}$ denote the transverse cylindrical polar coordinates about the SMF axis.

At the receiver end of the fibre, at $z = \ell$, the intensity distribution I of the NFP is given by

$$I(r, \phi, \ell) = \frac{1}{2} \text{Re} \{ \mathbf{E}(r, \phi, \ell) \times [\mathbf{H}(r, \phi, \ell)]^* \cdot \mathbf{u}_z \}. \quad (3)$$

So far, we have neglected the influence of DMA and mode mixing on the NFP. To simulate these effects, we employ a set of coupled power equations [7]

$$\frac{dP_\mu}{dz} = -\gamma_\mu P_\mu + \sum_{\nu} h_{\mu\nu} (P_\nu - P_\mu), \quad (4)$$

where P_μ and γ_μ are the power and the attenuation coefficient of the corresponding mode μ , respectively, and $\mu = \nu = 1, 2, 3, \dots$. The elements in the coupling matrix $h_{\mu\nu}$ are a measure of the probability per unit length of a transition occurring between modes μ and ν .

In order to reduce the set of coupled power equations in Eq. (4), we introduce principal mode groups (PMGs). PMGs are determined by the difference in the propagation coefficient between adjacent modes. If this difference is relatively small, modes belong to the same PMG. Consequently, mode mixing occurs between modes within a mode group, which is called intra-group mode mixing, and between mode groups themselves, called inter-group mode mixing. Since intra-group mode mixing is faster than the inter-group one, we may safely neglect the latter in short-range communication networks [5].

Further, we distinguish between a region near the launch end, where intra-group mode mixing is still negligible, a transition region and a region where intra-group mode mixing is at an advanced stage. In this latter region, it is acceptable to assume that the power within a mode group is approximately equally divided among the modes of the group. Since the modal amplitudes $A^{m,n}$ at $z = 0$ are known, the average amplitude of each mode in a PMG reads

$$|A_{PMG}^{m,n}|_{ave} = \sqrt{\frac{\sum_{m,n} |A_{PMG}^{m,n}|^2}{N_{PMG}}}, \quad (5)$$

where N_{PMG} denotes the amount of modes in a mode group. The phase of $A_{PMG}^{m,n}$ is chosen randomly, with a uniform distribution within $[0, 2\pi)$, as it is mixed in a random fashion with the other modes within the group. Moreover, the phase noise, due to the finite linewidth of the laser, also contributes to a random phase.

Since we have neglected the coupling between PMGs, the coupling matrix $h_{\mu,\nu}$ in Eq. (4) diagonalises, and consequently $P_\mu(z) = P_\mu(0) \exp(-\gamma_\mu z)$, where the index μ is now related to PMGs instead of separate modes. Note that we could have included the exponential as an imaginary part of $k_z^{m,n}$ in Eq. (1). However, then prior knowledge of the modes belonging to a PMG would have to be available. Under the weakly guiding approximation, we can use the concept of LP-modes, where a relation between the PMG and the modal indices exists. For an arbitrary index profile such relation is not available, and hence, computation of the real part of $k_z^{m,n}$ is necessary to distinguish between the PMGs. The γ_μ -dependence is added in the computation of the modal power.

For mode group μ , a matched formula for the attenuation coefficient γ_μ for silica fibres is given by [8]

$$\gamma(\mu, \lambda) = \gamma_0(\lambda) + \gamma_0(\lambda) I_\rho \left[\eta \left(\frac{\mu - 1}{M_{PMG}} \right)^{2\alpha/(\alpha+2)} \right], \quad (6)$$

where $\rho = 9$, $\eta = 7.35$, I_ρ denotes the modified Bessel function of order ρ , and γ_0 is the intrinsic fiber attenuation at a specific wavelength λ , which is equal for all PMGs. Further, M_{PMG} denotes the total number of PMGs, whereas α is the exponent of the graded-index power-law profile. Observe that the higher-order PMGs are attenuated more than the lower-order ones.

Experimental Results

A Fabry-Perot laser, with a central wavelength at $\lambda = 660\text{nm}$, is pigtailed to a 1m SMF. The SMF has a numerical aperture (NA) of 0.12 and a mode-field diameter of $4.2\mu\text{m}$. In order to excite the GI-MMF with a possible offset, a computer controlled set-up with transitional stages is used. The circularly symmetric GI-MMF has a core/cladding diameter of $62.5/125\mu\text{m}$, and $\text{NA}=0.275$. It is designed for use at $\lambda = 850\text{nm}$. Having performed several DMD simulations, the corresponding α -parameter of the graded-index profile is found to be $\alpha = 2.06$ [3]. At the receiver end of the fibre, the NFP is observed with a charge-coupled device (CCD) camera through a microscope.

For various radial offsets (r_0) and angular offsets (a_0), the simulated and measured NFPs at $z = 1\text{m}$ are shown in Figure 1. Intra-group mode mixing has not been included, which seems reasonable as the power has not yet been equally divided among the modes in a PMG. The measured and simulated intensity patterns look similar, which confirms that there is no significant mixing within the PMGs. Observe the ring-like shape of the field as we excite the GI-MMF with $r_0=13\mu\text{m}$ and $a_0=6.5^\circ$.

Next, we investigate the influence of intra-group mode mixing on the NFPs. In Figure 2(a), simulated and measured intensity patterns at $z = 75\text{m}$ and $z = 1\text{km}$ for $r_0=13\mu\text{m}$ are shown. We observe that mode mixing produces a more blurred simulated NFP compared to the ones in Figure 1. In Figure 2(b), an additional $a_0=6.5^\circ$ is inserted. At $z = 75\text{m}$ simulations and measurements are in good agreement. However, at $z = 1\text{km}$, the simulated fields move outward, which effect is absent in the measurements. Now, we recall that DMA attenuates the higher-order modes more than the lower-order ones. Simulation results at $z = 1\text{km}$ without and with DMA are shown in Figure 3. We see that with DMA the NFPs give a better agreement with the measurements in Figure 2.

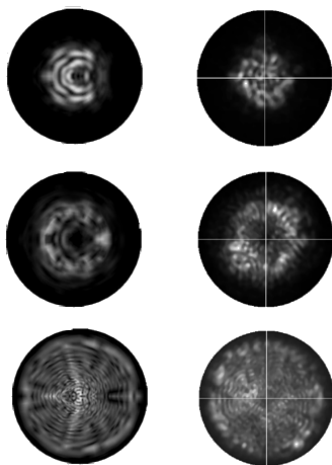


Figure 1: Simulations (left) and measurements (right) at $z = 1\text{m}$. Upper: $ro=13\mu\text{m}$; centre: $ro=13\mu\text{m}$ and $ao=6.5^\circ$; bottom: $ro=26\mu\text{m}$.

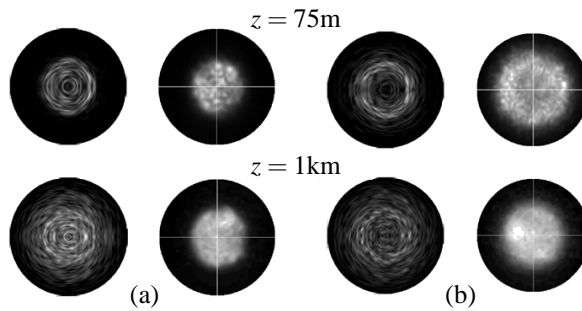


Figure 2: Simulations (left) and measurements (right) at $z = 75\text{m}$ and $z = 1\text{km}$ (a): for $ro=13\mu\text{m}$; (b): for $ro=13\mu\text{m}$ and $ao=6.5^\circ$.

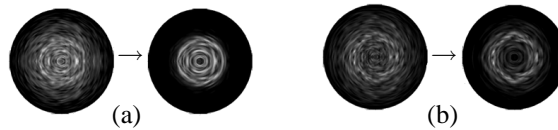


Figure 3: Simulations without (left) and with (right) DMA at $z = 1\text{km}$ for (a) $ro=13\mu\text{m}$; (b): $ro=13\mu\text{m}$ and $ao=6.5^\circ$.

Conclusions

We have developed a full-wave model to compute intensity patterns in a lossless circularly cylindrical MMF. A straightforward analysis shows that (intra-group) mode mixing and DMA can be easily implemented to obtain NFPs that are in reasonable agreement with measurements. We have performed these measurements with a GI-MMF, excited by a pigtailed SMF. For short GI-MMFs, intra-group mode mixing, in combination with possible phase noise, generate a blurry NFP. It is shown that DMA causes the higher-order modes to be attenuated more than the lower-order ones. By generating NFPs at several distances, we have gained insight in where these effects occur.

References

- [1] L. Raddatz, I.H. White, D.G. Cunningham and M.C. Nowell, "An Experimental and Theoretical Study of the Offset Launch Technique for the Enhancement of the Bandwidth of Multimode Fiber Links", *J. of Lightw. Techn.*, vol. 16, pp. 324-331, 1998.
- [2] T. Koonen, H. van den Boom, I.T. Monroy and G.D. Khoe, "High Capacity Multi-Service In-House Networks using Mode Group Diversity Multiplexing", in *Proceedings of OFC2004; Los Angeles, CA*, 2004, paper FG4.
- [3] M. Bingle and B.P. de Hon, "Differential Mode Delay - Full-Wave Modelling and Various Levels of Approximations", in *Proceedings of the XXVIIth General Assembly of the International Union of Radio Science; URSI, Maastricht*, vol. 24, 2002, pp. 1-4.
- [4] W. Hermann and D.U. Wiechert, "Refractive Index of Doped and Undoped PCVD Bulk Silica", *Mat. Res. Bull.*, vol. 24, pp. 1083-1097, 1989.
- [5] S. Kawakami and H. Tanj, "Evolution of Power Distribution in Graded-Index Fibres", *Electr. Lett.*, vol. 19, pp. 100-102, 1983.
- [6] E.G. Neumann, *Single-Mode Fibers, Fundamental*, Berlin: Springer, 1988, pp. 170-174.
- [7] D. Marcuse, *Theory of Dielectric Optical Waveguides, Sec. Ed.*, San Diego: Academic Press, 1991.
- [8] G. Yabre, "Comprehensive Theory of Dispersion in Graded-Index Optical Fibres", *J. of Lightw. Techn.*, vol. 18, pp. 166-176, 2000.